Available online at www.sciencedirect.com
SciVerse ScienceDirect
Ceramics International 39 (2013) 5271–5279
CERAMICS INTERNATIONAL
www.elsevier.com/locate/ceramint

Fabrication of AMCs by spray forming: Setting of cognition and social parameters to accelerate the convergence in optimization of spray forming process

Mohsen Ostad Shabani, Ali Mazahery*

Karaj Branch, Islamic Azad University, Karaj, Iran

Received 29 November 2012; received in revised form 6 December 2012; accepted 9 December 2012
Available online 20 December 2012

Abstract

Spray forming (also known as spray atomization and deposition) is of interest as a manufacturing technique that combines near-net-shape capabilities with the structural control available through rapid solidification. The present article focuses on development of a comprehensive method to optimize a number of parameters in the spray deposition processing of Al matrix composites including melt superheat, nozzle to substrate distance, metal to gas flow rate and high heat removal rate at the droplet–gas interface. The SiC particles reinforced Al matrix composites were produced by the spray atomization and co-deposition process using optimized parameters. Microscopic investigations of the composite specimens indicate that the distribution of SiC in the matrix alloy is fairly uniform. The wear rate and volume loss showed the two stages (run-in and steady state) of wear for all the applied loads. Microstructural analyses of the wear surfaces and debris were carried out in order to understand the wear mechanism.

Keywords: D. SiC particles; Al matrix; Wear

1. Introduction

The development in optimization theory has seen the emergence of a category of random search methods for solving global optimization problems [1–3]. Ant colony and particle swarm optimization are two paradigms of this kind of methods which are efficient tools for solving engineering problems [4–7]. The PSO algorithm was originally proposed by Kennedy as a simulation of social behavior of bird flock [8–10]. It can be easily implemented and is computationally inexpensive, since its memory and CPU speed requirements are low [11,12]. PSO has been proved to be an efficient approach for many continuous global optimization problems and in some cases it does not suffer the difficulties encountered by GA [13,14]. During the last decade, there has been a lot of remarkable developments in the field of PSO, particularly in improvements and applications of the algorithm [15].

Novel computational methods are used in some fields of engineering sciences, including the solidification and deformation of metal matrix composites (MMCs) in materials science [16–18]. The widespread use of cast discontinuous reinforced MMC applications in the industrial sector replaced most of the ferrous metal with its attractive physical and mechanical properties [19–24]. The MMC is noted to weigh less than the ferrous metal and still provides compatible mechanical properties [25–29]. Even though, aluminum alloys are promising structural materials due to their high specific strength and stiffness, their applications are restricted because of their poor wear resistance [30–36]. Aluminum metal matrix composites (AMCs) have drawn considerable attention as fuel efficient advance materials for tribological applications [37–41]. The desirable mechanical properties can be achieved by varying the reinforcing materials and their volume fraction in the composite [42–45]. The strength of the composite is mainly determined by the balance between the reinforcing particles sharing the load [46–48]. The elastic modulus of the composite is controlled by the volume percentage of

*Corresponding author. Tel.: +98 912 563 6709; fax: +98 261 6201888.
E-mail address: ali.mazahey@gmail.com (A. Mazahery).

0272-8842/$ - see front matter
http://dx.doi.org/10.1016/j.ceramint.2012.12.028

the reinforcing material, whereas the ductility, yield stress, and tensile strength are mainly affected by the matrix alloy and temper condition.

Many processing techniques have been developed successfully to manufacture MMCs (powder metallurgy, liquid metallurgy, diffusion bonding techniques, infiltration, squeeze casting, compocasting and spray deposition techniques) on the commercial scale [23–31]. The most simplified approach to develop near net shaped aluminum based composites is by liquid metallurgy route as it is economical and can result in mass production [22,25]. However, the study of cast aluminum containing particles Al_2O_3 and SiC showed settling of particulates in the sand mold [19]. This problem can be eliminated in spray forming process. It is a near net-shape processing technique combining atomization and deposition of liquid melt in single step, whereas the other P/M and ingot metallurgy routes contain large number of processing steps. Hence, the spray forming reduces the number of secondary processes and thus resulting in reduction of the production cost [20].

In this technique, the melt is atomized by high energy gas jet to generate spray of micron size droplets which is subsequently deposited on a stationary or movable substrate to consolidate into a near net shape preform. Rapid solidification effects inherent in spray deposition provide a substantial chemical and microstructural homogeneity together with refinement in grain size and second phase particle size.

The purpose of this study is to model and optimize the spray deposition process (melt superheat, nozzle to substrate distance, metal to gas flow rate and high heat removal rate at the droplet–gas interface) in order to refine the microstructure of the wear resistant aluminum–SiC composites and improve the uniformity in distribution of reinforcement in the matrix. The basic physics involved are: (1) the fragmentation of a continuous liquid stream into discrete droplets; (2) multi-phase flow of the gas-droplet spray cone and non-linear heat transfer; (3) droplet deposition, splashing and re-deposition; and (4) preform solidification and microstructure evolution.

2. Particle swarm optimization

2.1. Classical PSO

PSO was first introduced by Kennedy and Eberhart [3–7]. PSO employs a population of particles that fly over the fitness landscape, of which the swarm dynamics is inspired by the collective behavior of organisms, such as bird flocking and fish schooling. Each particle holds a memory of the best position that it has seen so far and the best position obtained within its neighborhood. A particle updates its velocity based on its current velocity and position along with the above two memorized positions. The modification of the moving orbit of a particle (particle i) is described as follows [11,12]:

$$V_{i,j}^{t+1} = wV_{i,j}^{t} + c_1 r_{1i,j}^{t}(p_{ij}^{t} - x_{ij}^{t}) + c_2 r_{2_{i,j}}^{t}(Q_{ij}^{t} - X_{ij}^{t}) \quad (1)$$

$$X_{i,j}^{t+1} = V_{i,j}^{t+1} + X_{i,j}^{t} \quad (2)$$

where c_1 and c_2 are two positive constants, known as the acceleration coefficients; r_1 and r_2 are two uniformly distributed random numbers on the range (0,1) for the jth dimension of particle i. Vector $p_i=(p_{i1}^t, p_{i2}^t \ldots\ p_{iD}^t)$ is the position with the best fitness found so far for the ith particle, which is called personal best (p_{best}) position. And vector $Q_i=(Q_1^t, p_2^t \ldots\ p_D^t)$ records the best position discovered by the swarm so far, known as the global best (g_{best}) position. $x_{i,j}^t$, $v_{i,j}^t$ and $p_{i,j}^t$ are the jth dimension of vector of xi^t, $v_{i,}^t$ and $p_{i,}^t$, respectively. The parameter w is the inertia weight used for the balance between the global and local search abilities.

In the classical PSO model, according to Eqs. (1) and (2), particles share information through the swarm attractor, Q_i, and evoke memories via particle attractors, p_i [49–51]. Based on Eqs. (1) and (2), each particle's movement can also be considered as being accelerated by two elastic forces produced by two attractors, which correspond to the previous best position found by itself and the previous best position found by particles in its neighborhood, respectively. Several versions of the PSO algorithm have been developed [52–54]. Among them, there are two main models, called g_{best} (global best) and l_{best} (local best), respectively. These two models differ in the way of defining the neighborhood for each particle. In the g_{best} model, the neighborhood of a particle consists of the particles in the whole swarm, which share information between each other. On the contrary, in the l_{best} model, the neighborhood of a particle consists of several fixed particles.

2.2. SRPSO

The proposed selective regenerated particle swarm optimization (SRPSO) aims at improving the original PSO. Two new features are designed. A suggestion on the setting of cognition and social parameters, c_1 and c_2, is proposed to accelerate the convergence. In addition, a selective particle regeneration mechanism for avoiding the search trapped in local optima.

As shown in Eq. (1), the new velocity of a particle is determined based on the best individual position and the knowledge of the swarm's best. $(P_i - x_i)$ represents the cognitive knowledge and $(Q_i - x_i)$ corresponds to the social knowledge. Their relative effect on the new velocity is determined by the respective weights of parameter c_1 and c_2. As recommended by Kennedy [11], these two parameters are typically assigned the same value. As a result, the next position of a particle is usually the middle of P_i and Q_i, as illustrated in Fig. 1. In that case, it may take more iterations for the particle to move closer to the global best location and thus affect the efficiency of the search. In order to accelerate the convergence, it is suggested that a larger value should be assigned to c_2 with respect to c_1 [14]. Consequently, the new

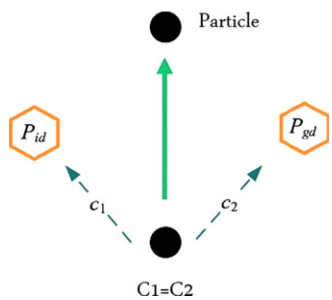

Fig. 1. Particle moving behavior when the two parameters are typically assigned the same value.

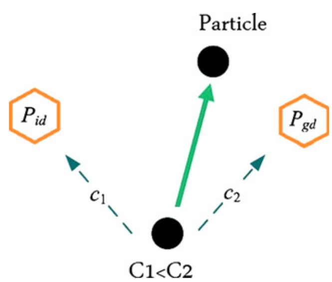

Fig. 2. Particle moving behavior when C1 < C2.

position of a particle will be closer to the global best location, Q_i. The concept is illustrated in Fig. 2. With the suggested setting, the convergence of particles will be accelerated.

The unbalanced setting of c_1 and c_2 is able to accelerate convergence, but it also increases the probability that particles are more easily trapped in local optima. In order to prevent premature convergence, a novel mechanism "selective particle regeneration" is designed. The idea is to select particles that are likely trapped and re-assign their new positions with certain degrees of randomness as an attempt to escape from local optimum. It is equivalent to eliminating those particles that are selected and in the mean time regenerate the same number of particles with random positions.

More specifically, there are two major operations in this mechanism, particle selection and particle regeneration. In each iteration, a portion of the particles in the swarm with current positions very close to the global best position are selected for regeneration since they are more likely to move around and closer to the current global best particle and will not further contribute to the search [4–10]. By reposition those particles far away from the global best particle, they will be able to search new areas and thus increase the chances to find better solutions. Note that the current global best particle will not be selected for generation so that the current best solution is preserved. New positions of the chosen particles are not determined by applying Eqs. (1) and (2). The assignment of new positions contains random factors in order for the selected particles to jump out of local regions. In the mean time, it also involves knowledge of the swarm for the purpose of preserving valuable information.

Clustering is a common problem in statistical data analysis, which can be seen in many fields, including machine learning, data mining, pattern recognition, image analysis and bioinformatics. The *K*-means clustering algorithm was developed by Hartigan which is one of early and simple clustering approach. It applies partitional technique to determine the clustering result through iterative hill climbing. First, users determine the number of cluster centroids, *k*. After that, the *K*-means algorithm classifies data points into clusters base on the Euclidean distance calculation. The procedure of the *K*-means algorithm is described as follows:

(I) Initiation
(II) Clustering
(III) Calculation of centroid
(IV) Stop

SRPSO can also be applied to data clustering problems with the same encoding method as mentioned above. In addition, a hybrid algorithm that combines *K*-means and SRPSO is developed. *K*-means has the advantage of being a very efficient local search procedure but its convergence is extremely sensitive to the chosen initial solution. SRPSO belongs to the class of global search procedures but requires much computational effort. The goal of integrating *K*-means and SRPSO is to combine their advantages while avoiding their shortcomings. This hybrid algorithm first executes the *K*-means algorithm. The outcome of *K*-means serves as one of the particles in the initial solution of SRPSO.

3. Optimized parameters

Experiments were conducted in order to determine the best parameter values for the proposed algorithm. As SRPSO is to be applied to clustering problems with high-dimensional datasets, the dataset Wine, is selected for the experiments. The main effects function of Minitab is applied to analyze the interaction effect and calculate appropriate combination of parameter values. PSO performs well in this dataset with an average value that are very close to the optimal value and a very small standard deviation. *K*-means, however, yields a larger average values and exhibit large variation between runs. *K*-means reaches local optima very quickly but shows no further movement. As a result, the obtained solutions may not be of high quality. PSO displays the ability of jumping out of local optima and moving toward better solutions. Compared to PSO, the three figures clearly show that SRPSO has similar capability of escaping from local optima, but finds the same or better values with less numbers of iterations. It demonstrates that the suggested unbalanced parameter setting enables SRPSO faster convergence while the particle regeneration mechanism prevents trapping it in local optima. KSRPSO, on the other hand, exhibits both the advantages of *K*-means and SRPSO. Like *K*-means, KSRPSO leaps to a local optimal value very quickly but it also shows the ability of improving current best solutions. Fig. 3 shows the effect of iteration number on the root mean square (RMS) error of developed model. The numbers of iteration were selected to be 50,000.

KSRPSO is employed for optimization of parameters in this study. Spray forming consists of the sequential steps: (1) atomization of liquid materials to create a droplet spray; (2) control of the resulting droplet spray in the gas flow field to achieve a desired droplet mass and enthalpy distribution prior to deposition; and (3) the deposition of droplets at a surface to build up a pre-defined perform. Final optimized parameters are 115 μm particulate size, 2 kg weight of the charge, 710 °C melt temperature, 320 mm nozzle to substrate distance, 10 mm inner diameter of melt delivery tube, 100 kg cm^{-2} nitrogen gas pressure, 1.2 mm injector orifice diameter.

4. Optimized experimental procedure

In this study, SiC particles Al matrix composites were produced by the spray atomization and co-deposition process. The chemical composition of Al–Si alloy is given in Table 1. In brief the process employs an annular spray nozzle with convergent–divergent configuration. In this process, the gas melt interaction occurs at the tip of a flow tube concentric to gas flow channel to promote atomization of the melt. The melting of the alloy was carried out in a graphite crucible in a resistance heating furnace at 750 °C. After cooling the melt to 710 °C, it is poured in the convergent–divergent nozzle assembly. Before pouring high pressure nitrogen gas is allowed to pass through the divergent section of the nozzle. The aerodynamic forces exerted by high velocity nitrogen gas jets atomize the molten metal stream into fine droplets. Injectors are used to incorporate SiC particles in the spray cone. The droplets get solidified and build up preform of diameter 150 mm. For wear testing, the samples were cut from different areas of the preform. The X-ray diffraction patterns of the prepared sample was recorded. The collected data were matched with reference data for identification of different phases.

Dry sliding wear tests of the reinforced and unreinforced alloys have been performed under the ambient temperatures between 25 and 30 °C and relative humidity between 25% and 42%, using a pin-on-disc wear and friction monitor. The cylindrical shaped samples of base Al alloy and spray formed Al–SiC composite were tested against the hardened EN32 steel disc having chemical composition (0.14% C, 0.52% Mn, 0.18% Si, 0.13% Ni, 0.05% Cr, 0.06% Mo, 0.019% P, 0.015% S, and balance Fe) and hardness 65 HRC. Before testing, each specimen is ultrasonically cleaned in acetone. Wear rate has been calculated by measuring weight loss at different time intervals. The scanning electron microscope is used for microstructural examination of specimen, analyzing worn surfaces, and debris collected during the test.

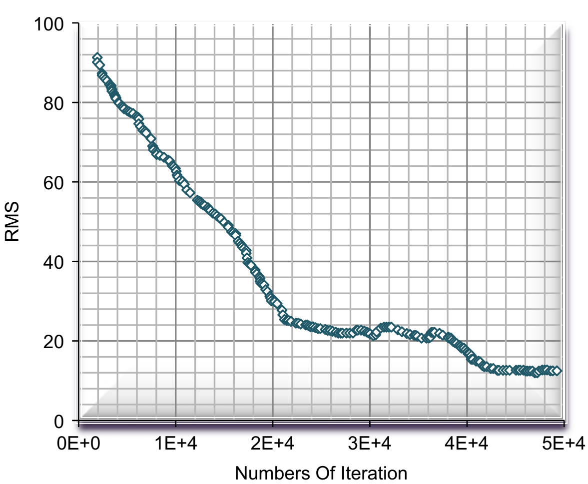

Fig. 3. The effect of iteration number on the RMS.

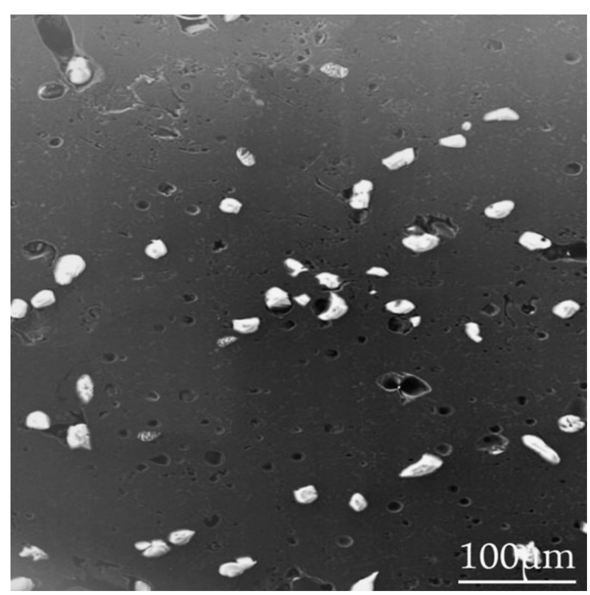

Fig. 4. SEM microphotograph of sprayed Al–SiC composites.

Table 1
Chemical composition of Al–Si alloy.

Si	Fe	Cu	Mn	Mg	Zn	Ti	Cr	Ni	Pb	Sn
6.91	0.4	0.25	0.2	0.33	0.31	0.02	0.01	0.05	0.1	< 0.01

5. Optimized experimental results

The homogenous distribution of the reinforcement phase is an essential condition for a composite material to achieve its superior performance. Particularly in the case of discontinuous aluminum matrix composites, the homogeneous distribution of the reinforcing phase is an essential requirement. Fig. 4 shows a typical SEM microphotograph of sprayed Al–SiC composites. The SiC particles are angular in shape and distributed homogeneously throughout the Al matrix. The XRD pattern of the SiC reinforced Al matrix composites is displayed in Fig. 5. It can be seen that SiC and aluminum are present and no other reaction products are formed in the system.

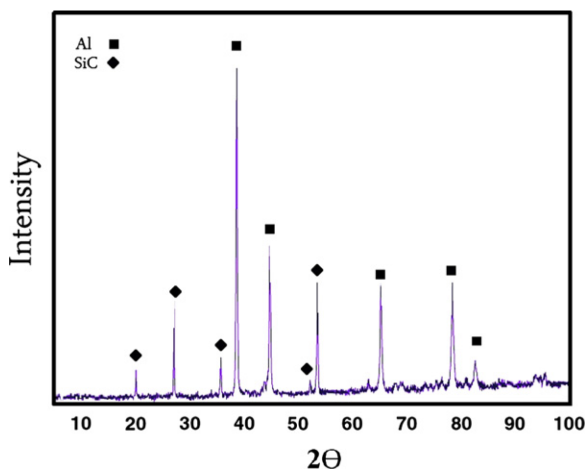

Fig. 5. The XRD pattern of the SiC reinforced Al matrix composites.

Tribological properties of aluminum matrix composites is of great interest. The plastic deformations are unwelcome and represent the limiting factor for tribological application of these materials. The wear rate behavior against sliding distance has been recorded at each load for both base Al alloy and Al/SiC composites (Fig. 6). Wear rate was found to increase with increasing the applied loads. Similar findings have been also reported by previous investigators [20,41]. At every load, the composite material offers greater resistance to wear than base Al–Si alloy. The most significant difference in wear rates of the composites have been found at higher loads. This resistance to wear is catered by harder particle reinforced in the softer Al–Si alloy matrix offering more obstacles for the dislocations to propagate through the matrix. Improvement in the wear resistance of the composites can be also attributed to the formation of mechanically mixed layers (MML) consisting of oxides of iron and aluminum during sliding of composites on hard steel surfaces. The MML poses a greater resistance to the sliding wear and friction as it reduces the extent of direct metal to metal contact. The formation of MML is resulted from the oxidation of the exposed metal surface in the relative motion. The rupture of the oxide layer during transversal and reoxidation of exposed metal surface is called oxidation–delamination–reoxidation. Moreover, the compaction of the debris between the sliding surfaces favored the development of wear protective oxide layer. It is observed that under an applied load two different type of wear behavior can be predicted from the curves (run-in and steady state wear rates). Fluctuating, unstable and greater wear at the initial stage corresponds to the run-in wear. On the other hand, constant

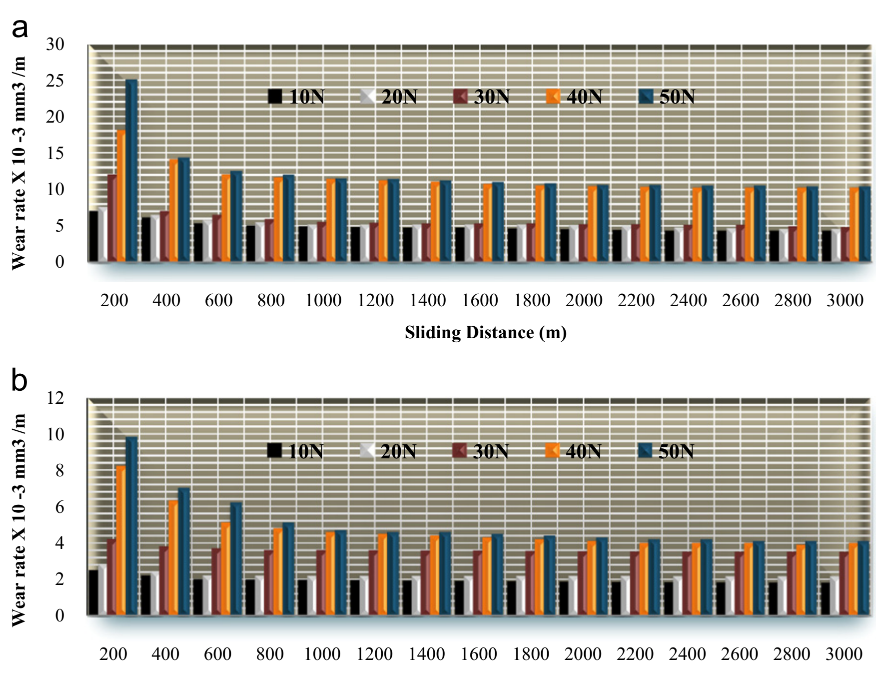

Fig. 6. The wear rate behavior versus sliding distance: (a) base Al alloy and (b) Al/SiC composites.

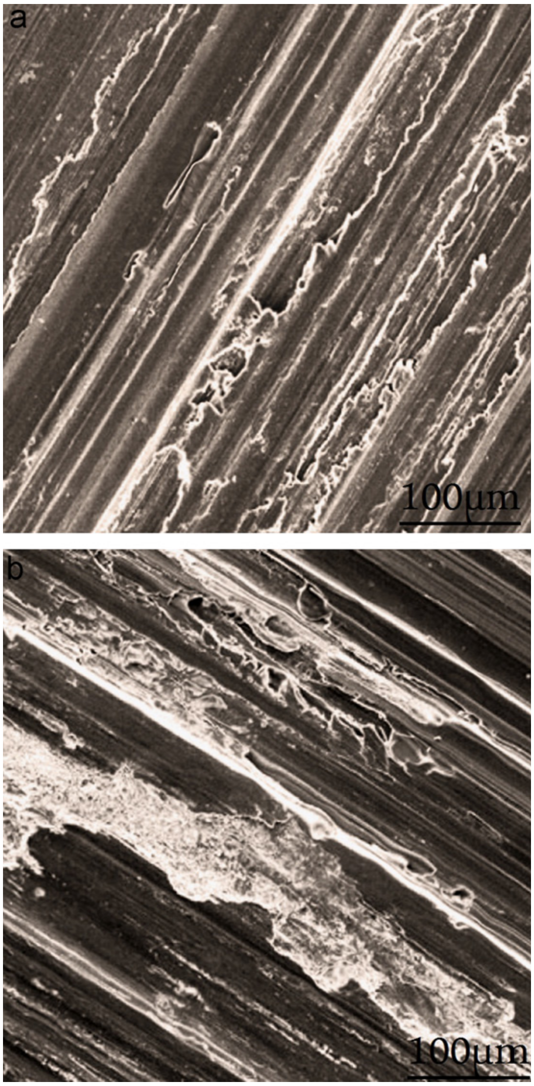

Fig. 7. The worn surfaces of Al base alloy at applied loads of: (a) 20 and (b) 50 N.

wear rate has been obtained at later stage corresponding steady state wear. For both reinforced and unreinforced materials, a steady state is approachable after 1 km sliding distance for all applied loads.

The worn surfaces of Al base alloy (at 20 and 50 N loads) have been shown in Fig. 7. One of the common features observed in both lower and higher load, is the formation of grooves and ridges running parallel to the sliding direction in both base alloy. These wear scars are the primarily characteristic of abrasive wear. It has been found that grooves are fine on the worn surface of Al alloy subjected to 20 N load in comparison to 50 N load. Fig. 8 shows the worn surfaces of composite at applied loads of 20, 30 and 50 N. The amount of repetitive micro-ploughing and material removal of the soft alloy by hard steel counterpart can be seen in Fig. 8. The depth of micro-ploughing is increased by increasing load where contact asperities change the shape. Thus, the size and depth of the grooves become greater at this stage.

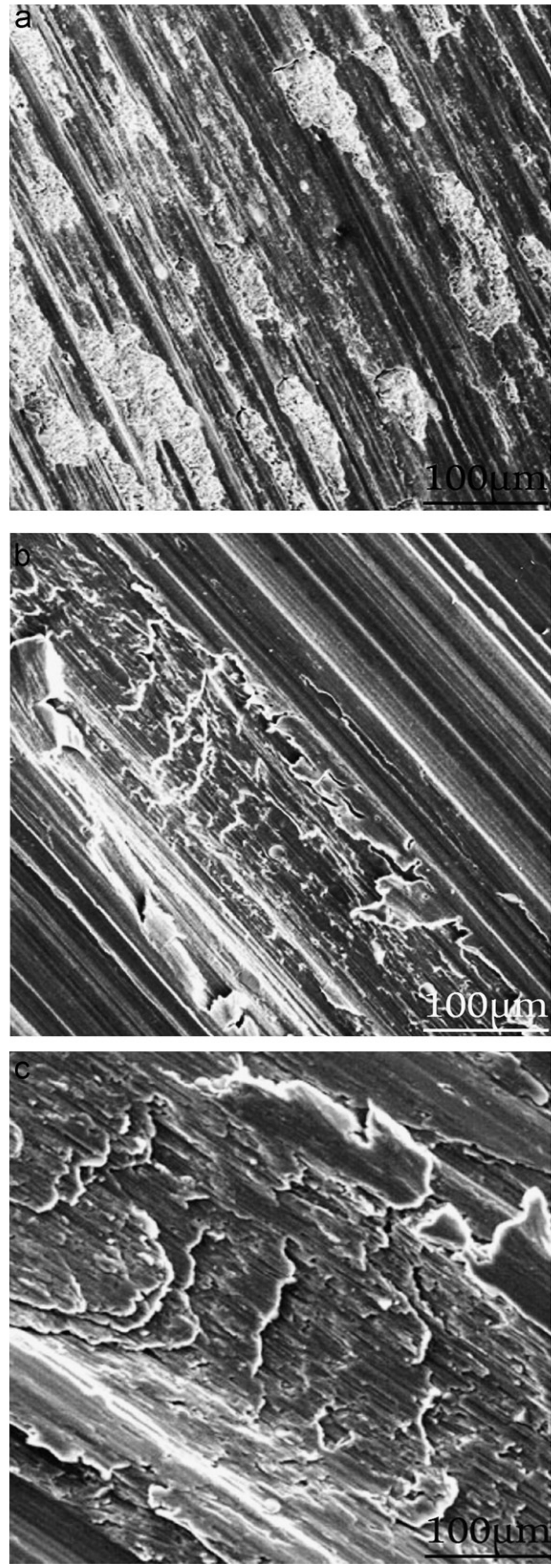

Fig. 8. The worn surfaces of composites at applied loads of: (a) 20, (b) 30 and (c) 50 N.

Debris formation can be seen from the ridge as the crack propagates perpendicular to the sliding direction in Al alloy. Fig. 9 displays the worn debris of the base Al alloy and the composite. Smaller sized wear debris are observed in the

Fig. 9. The worn debris of: (a) base Al alloy and (b) the composite.

composite as compared to the base Al alloy. It can be further related to the greater resistance to the seizure and different wear mechanisms offered by composite material as compared to base Al alloy. Fig. 10 shows the efficacy of the optimization scheme by comparing the predicted results with the experimental values. There is a convincing agreement between experimental values and predicted values for wear rate of SiC particles reinforced Al matrix composites

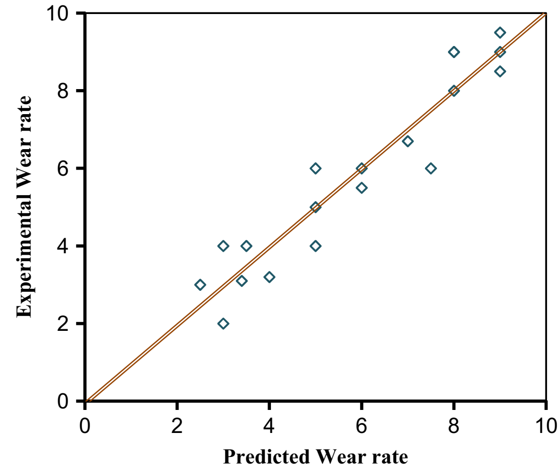

Fig. 10. Comparison between the experimental and predicted values of Wear rate.

6. Conclusion

It is concluded that the novel technique implemented in this investigation could provide quantitative guidance for the optimization of the spray forming process in terms of preform shape, microstructure and overall economic performance.

Therefore, this work shows the usefulness of an intelligent way to predict the performance of Al matrix composites using selective regenerated particle swarm optimization. Experimental investigation shows that the wear resistance offered by spray processed composite is higher than base Al alloy with incorporation of harder phase which is the result of good interfacial bonding of SiC particle and matrix phase. Four different morphological features are observed on the worn surfaces; metal flow lines, micro-ploughing, propagation of cracks at the periphery of the crater, and detachment of debris. Moreover, the mechanically welded layer is also being observed on the worn surfaces due to the transfer of counterpart steel disc. It is noted that material is removed in the form of debris from rubbing surfaces during micro-ploughing. In the composite most of the material gets displaced on the sides of grooves due to plastic deformation.

References

[1] J.J. Liang, A.K. Qin, P.N. Suganthan, S. Baskar, Comprehensive learning particle swarm optimizer for global optimization of multimodal functions, IEEE Transactions on Evolutionary Computation 10 (2006) 281–295.
[2] M.O. Shabani, A. Mazahery, The ANN application in FEM modeling of mechanical properties of Al–Si alloy, Applied Mathematical Modelling 35 (2011) 5707–5713.
[3] J. Kennedy, R.C. Eberhart, Particle swarm optimization, in: Proceedings of the IEEE International Conference on Neural Networks, vol. IV, Perth, Australia, (1995), pp. 1942–1948.
[4] A.P. Engelbrecht, B.S. Masiye, G. Pampara, Niching ability of basic particle swarm optimization algorithms, in: Proceedings of the IEEE Swarm Intelligence Symposium, (2005).
[5] A. Mazahery, M.O. Shabani, Process conditions optimization in Al–Cu alloys matrix composites, Powder Technology 225 (2012) 101–106.
[6] R.A. Krohling, E. Mendel, Bare bones particle swarm optimization with Gaussian or Cauchy jumps, in: Processing of the IEEE Congress on Evolutionary Computation, (2009), (CEC'09), pp. 3285–3291.
[7] M.O. Shabani, A. Mazahery, Artificial Intelligence in numerical modeling of nano sized ceramic particulates reinforced metal matrix composites, Applied Mathematical Modelling 36 (2012) 5455–5465.

[8] D. Beasley, D.R. Bull, R.R. Martin, A sequential niching technique for multimodal function optimization, Evolutionary Computing 1 (2) (1993) 101–125.

[9] R. Brits, Niching Strategies for Particle Swarm Optimization, Master's Thesis, Department of Computer Science, University of Pretoria, Pretoria, South Africa, November 2002.

[10] M.O. Shabani, A. Mazahery, Application of FEM and ANN in characterization of Al Matrix nano-composites using various training algorithms, Metallurgical and Materials Transactions A 43 (2012) 2158–2165.

[11] J. Kennedy, Small worlds and mega-minds: effects of neighborhood topology on particle swarm performance, in: Proceedings of the IEEE Congress on Evolutionary Computation, July 1999, pp. 1931–1938.

[12] A. Mazahery, M.O. Shabani, A356 reinforced with nano particles: Numerical analysis of mechanical properties, JOM: Journal of the Minerals, Metals & Materials 64 (2) (2012) 323–329.

[13] J. Kennedy, R.C. Eberhart, Swarm Intelligence, Morgan Kaufman, (2001).

[14] J. Kennedy, R. Mendes, Population structure and particle swarm performance, in: Proceedings of the IEEE World Congress on Evolutionary Computation, Honolulu, Hawaii, May 2002, pp. 1671–1676.

[15] F. van den Bergh, A.P. Engelbrecht, A study of particle swarm optimization particle trajectories, Information Science 176 (8) (2006) 937–971.

[16] M.O. Shabani, A. Mazahery, The synthesis of the particulates Al matrix composites by the compocasting method, Ceramics International 39 (2013) 1351–1358.

[17] R. Bauri, M.K. Surappa, Processing and compressive strength of Al–Li–SiCp composites fabricated by compound billet technique, Journal of Material Processing Technology 209 (2009) 2077–2084.

[18] M.O. Shabani, A. Mazahery, Optimization of process conditions in casting aluminum matrix composites via interconnection of artificial neurons and progressive solutions, Ceramics International 38 (2012) 4541–4547.

[19] J. Hashim, L. Looney, M.S.J. Hashmi, Particle distribution in cast metal matrix composites. Part I, Journal of Materials Processing Technology 123 (2002) 251–257.

[20] A. Mazahery, M.O. Shabani, Tribological behaviour of semisolid–semisolid compocast Al–Si matrix composites reinforced with TiB2 coated B4C particulates, Ceramics International 38 (2012) 1887–1895.

[21] W.R. Blumenthal, G.T. Gray, T.N. Claytor, Response of aluminium-infiltrated boron carbide cermets to shock wave loading, Journal of Materials Science 29 (1994) 4567.

[22] M.O. Shabani, A. Mazahery, The performance of various artificial neurons interconnections in the modelling and experimental manufacturing of the composits, Materiali in Tehnologije 46 (2) (2012) 109–113.

[23] A.J. Pyzik, I.A. Aksay, Processing of ceramic and metal matrix composites, in: Proceedings of the International Symposium on Advances in: Processing of Ceramic and Metal Matrix Composites, New York, NY, (1989), p. 269.

[24] A. Mazahery, M.O. Shabani, Influence of the hard coated B4C particulates on wear resistance of Al–Cu alloys, Composites: Part B 43 (2012) 1302–1308.

[25] S.K. Rhee, Wetting of AlN and TiC by liquid Ag and liquid Cu, Journal of the American Ceramic Society 53 (1970) 386.

[26] M.O. Shabani, A. Mazahery, Prediction performance of various numerical model training algorithms in solidification process of A356 matrix composites, Indian Journal of Engineering & Materials Sciences 19 (2012) 129–134.

[27] M. Razavi, M.R. Rahimipour, R. Kaboli, Synthesis of TiC nanocomposite powder from impure TiO_2 and carbon black by mechanically activated sintering, Journal of Alloys and Compounds 460 (2008) 694–698.

[28] G.A. Irons, K. Owusu-Boahen, Settling and clustering of silicon carbide particles in aluminium metal matrix composites, Metallurgical and Materials Transactions B 26 (1995) 980–981.

[29] M.O. Shabani, A. Mazahery, The GA Optimization Performance in the Microstructure and Mechanical Properties of MMNCs, Transactions of the Indian Institute of Metals 65 (1) (2012) 77–83.

[30] M. Gupta, L. Lu, S.E. Ang, Effect of microstructural features on the aging behaviour of Al–Cu/SiC metal matrix composites processed using casting and rheocasting routes, Journal of Materials Science 32 (1997) 1261–1267.

[31] P.A. Karnezis, G. Durrant, B. Cantor, Characterization of reinforcement distribution in cast Al-alloy/SiC composites, Materials Characterization 40 (1998) 97–109.

[32] A. Mazahery, M.O. Shabani, Study on microstructure and abrasive wear behavior of sintered Al matrix composites, Ceramics International 38 (5) (2012) 4263–4269.

[33] C.J. Quaak, W.H. Kool, Properties of semisolid aluminium matrix composites, Materials Science and Engineering A 188 (1994) 277–282.

[34] M.O. Shabani, A. Mazahery, Prediction of mechanical properties of cast A356 alloy as a function of microstructure and cooling rate, Archives of Metallurgy and Materials 56 (3) (2011) 671–675.

[35] A.J. Asthana, Reinforced cast metals, part II evolution of the interface, Journal of Material Science and Engineering 35 (1998) 1959–1980.

[36] C.A. Leon, R.L. Drew, Preparation of nickel-coated powders as precursors to reinforced metal matrix composites, Journal of Materials Science 35 (2000) 4763–4768.

[37] A. Mazahery, M.O. Shabani, Mechanical properties of squeeze-cast A356 composites reinforced with B 4C particulates, Journal of Materials Engineering and Performance 21 (2) (2012) 247–252.

[38] L.M. Tham, M. Gupta, L. Cheng, Effect of limited matrix–reinforcement interfacial reaction on enhancing the mechanical properties of aluminium–silicon carbide composites, Acta Materialia 49 (2001) 3243–3253.

[39] M.O. Shabani, A. Mazahery, Application of GA to optimize the process conditions of Al matrix nano-composites, Composites: Part B 45 (2013) 185–191.

[40] S.K. Thakur, B.K. Dhinan, The influence of interfacial characteristics between SiCp and Mg/Al metal matrix on wear, coefficient of friction and microhardness, Wear 247 (2001) 201.

[41] S.F. Moustafa, S.A.L. Badry, A.M. Sanad, B. Kieback, Friction and wear behavior of graphite–copper composites, Wear 253 (2002) 699–710.

[42] A. Mazahery, M.O. Shabani, The accuracy of various training algorithms in tribological behavior modeling of A356-B 4C composites, Russian Metallurgy (Metally) 7 (2011) 699–707.

[43] U. Cocen, K. Onel, Ductility and strength extruded aluminum alloy composites, Composite Science Technology 62 (2002) 275–282.

[44] M. McKimpson, T. Scott, Processing and properties of metal matrix composites containing discontinuous reinforcement, Materials Science and Engineering 107 (1989) 93–106.

[45] A. Mazahery, M.O. Shabani, A comparative study on abrasive wear behavior of semisolid–liquid processed Al–Si matrix reinforced with coated B4C Reinforcement, Transactions of the Indian Institute of Metals 65 (2) (2012) 145–154.

[46] V.K. Varma, S.V. Kamath, V.V. Kutumabarao, Tensile bahviour of powder metallurgy processed (Al–Cu–Mg)/SiCp composites, Material Science and Technology 17 (2000) 921–936.

[47] L. Zhong, Deformation behavior and microstructure effect in 2124Al/SiCp, Composites Journal of Composite Materials 34 (2000) 101–115.

[48] M.O. Shabani, A. Mazahery, Microstructural prediction of cast A356 alloy as a function of cooling rate, JOM: Journal of the Minerals, Metals & Materials 63 (8) (2011) 132–136.

[49] Y.G. Petalas, C.G. Antonopoulos, T.C. Bountis, M.N. Vrahatis, Detecting resonances in conservative maps using evolutionary algorithms, Physics Letters A 373 (2009) 334–341.

[50] A. Mazahery, M.O. Shabani, Assistance of novel artificial intelligence in optimization of aluminum matrix nanocomposite by genetic algorithm, Metallurgical and Materials Transactions A 43 (2012) 5279–5285.

[51] C.H. Wu, N. Dong, W.H. Ip, C.Y. Chen, K.L. Yung, Z.Q. Chen, Chaotic hybrid algorithm and its application in circle detection, Lecture Notes in Computer Science 6024 (2010) 302–311.

[52] M.O. Shabani, M. Alizadeh, A. Mazahery, Modelling of mechanical properties of cast A356 alloy, Fatigue & Fracture of Engineering Materials & Structures 34 (2011) 1035–1040.

[53] S.Z. Zhao, P.N. Suganthan, Two-lbests based multi-objective particle swarm optimizer, Engineering Optimization 43 (1) (2011) 1–17.

[54] P. Sathiya, S. Aravindan, A.N. Haq, K. Paneerselvam, Optimization of friction welding parameters using evolutionary computational techniques, Journal of Materials Processing Technology 209 (2009) 2576–2584.